How does the OH reactivity affect the ozone production efficiency: case studies in Beijing and Heshan, China

Yudong Yang[1], Min Shao[1, *], Stephan. Keβel[2], Yue Li[1], Keding Lu[1], Sihua Lu[1], Jonathan Williams[2], Yuanhang Zhang[1], Liming Zeng[1], Anke C. Nölscher[2, #], Yusheng Wu[1], Xuemei Wang[3], Junyu Zheng[4],

[1] State Joint Key Laboratory of Environmental Simulation and Pollution Control, College of Environmental Science and Engineering, Peking University, Beijing, China
[2] Department of Atmospheric Chemistry, Max Plank-Institute for Chemistry, Mainz, Germany
[3] School of Atmospheric Science, Sun Yat-Sen University, Guangzhou, China
[4] School of Environmental Science and Engineering, South China University of Technology, China
now at: Division of Geological and Planetary Sciences, California Institute of Technology, Pasadena, USA

* Corresponding to: Min Shao
Email address: mshao@pku.edu.cn

Abstract

Total OH reactivity measurements were conducted on the Peking University campus, Beijing in August 2013 and in Heshan, Guangdong Province from October to November 2014. The daily median OH reactivity were 20 ± 11 s^{-1} in Beijing and 31 ± 20 s^{-1} in Heshan respectively. The data in Beijing showed a distinct diurnal pattern with the maxima over 27 s^{-1} in early morning and minima below 16 s^{-1} in the afternoon. The diurnal pattern in Heshan was not as evident as in Beijing. Missing reactivity, defined as the difference between measured and calculated OH reactivity, was observed at both sites, with 21% missing in Beijing and 32% missing in Heshan. Unmeasured primary species, such as branched-alkenes could contribute to missing reactivity in Beijing, especially in morning rush hours. An observation-based model with the RACM-2 (Regional Atmospheric Chemical Mechanism version 2) was used to understand the daytime missing reactivity in Beijing by adding unmeasured oxygenated volatile organic compounds and simulated intermediates of the degradation from primary VOCs. However, the model could not find the convincing

explanation for the missing in Heshan, where the ambient air was found to be more aged, and the missing reactivity was presumably attributed to oxidized species, such as unmeasured aldehydes, acids and di-carbonyls. The ozone production efficiency was 21% higher in Beijing and 30% higher in Heshan when the model was constrained by the measured reactivity, compared to the calculations with measured and modeled species included, indicating the importance of quantifying the OH reactivity for better understanding ozone chemistry.

1. Introduction

Studies on total OH reactivity in the atmosphere have been of increasing interest over the last two decades. The instantaneous total OH reactivity, is defined as

$$k_{OH} = \sum_i k_{OH+X_i}[X_i] \quad (1\text{-}1)$$

where X represents a reactive species (CO, NO_2 etc.) and k_{OH+X_i} is the rate coefficient for the reaction between X and OH radicals. Total OH reactivity is an index for evaluating the amounts of reductive pollutants in terms of ambient OH loss and hence their roles in atmospheric oxidation (Williams, 2008; Williams and Brune, 2015; Yang et al., 2016). It also provides a constraint for OH budget calculation in both field campaigns and laboratory studies (Stone et al., 2012; Fuchs et al., 2013).

Total OH reactivity measuring techniques, e.g., two laser-induced-fluorescence (LIF) based techniques (Calpini, et al., 1999; Kovacs and Brune, 2001) and one proton-transfer-reaction mass spectrometry (PTR-MS) based technique, comparative reactivity method (CRM) (Sinha et al., 2008) were developed in recent years. A brief comparison of these techniques and their interferences were summarized (Yang et al., 2016). By deploying these measuring techniques, total OH reactivity measurements have been intensively conducted in urban and suburban areas. Details of these campaigns were listed in Table 1 and Table 2. Most of the campaigns exhibited similar diel features with higher reactivity in dawn and rush hours of early morning, and lower levels in the afternoon, which could be explained by the change in

boundary layer height, emissions and oxidation processes. Anthropogenic volatile organic compounds (VOCs) and inorganics, such as CO and NO_x (NO + NO_2) are major known OH sinks in urban areas.

However, a substantial difference between measured and calculated or modelled OH reactivity, termed as the missing reactivity, was revealed in most field campaigns. Compared to the high percentages of missing reactivity in forested areas (Sinha et al., 2010; Nölscher et al., 2012; 2016; Edwards et al., 2013, Williams et al., 2016), most campaigns in urban and suburban areas gave relatively lower percentages of missing reactivity except for the 75% missing reactivity in Paris in MEGAPOLI under the influences of continental air masses (Dolgorouky et al, 2012).

Various methods were used in exploring the origins of missing reactivity. Unmeasured primary species are important candidates. Sheehy et al. (2010) discovered a higher percentage of missing reactivity in morning rush hours and found that the unmeasured primary species, including organics with semi and low-volatility, could contribute up to 10% of total reactivity. Direct measurements on reactivity of anthropogenic emission sources were conducted, such as vehicle exhaust and gasoline evaporation. An average of 17.5% missing reactivity was found in vehicle exhaust measurements (Nakashima et al., 2010). For gasoline evaporation, a study showed that if primary emitted branched-chained alkenes were considered, the measured and calculated reactivity then agreed (Wu et al., 2015). Besides primary emitted species, unknown secondary species were not negligible. Yoshino et al. (2006) found a good correlation between missing reactivity and measured oxygenated VOCs (OVOCs) in three seasons except for winter, assuming that the unmeasured OVOCs could be major contributors of missing reactivity, in one case the OVOCs could increase reactivity by over 50% (Lou et al., 2010). The observation-based model (OBM) was widely used to evaluate the measured reactivity (Lee et al., 2010; Lou et al., 2010; Whalley et al., 2016), confirming the important contribution from OVOCs and undetected intermediate compounds,.

Ground-level ozone pollution has been of increasing concerns in China. While the ozone concentration exceeds Grade II of China National Ambient Air Quality

Standards (2012) (93 ppbV) frequently in summer in Beijing-Tianjin-Hebei area and Pearl River Delta (PRD) region (Wang et al., 2006; Zhang et al., 2008), it appears there is an increasing trend for ozone in Beijing and other area recent years (Zhao et al., 2009; Zhang et al., 2014). Comparing to traditional empirical kinetic model approach (EKMA) (Dodge et al., 1977), the OH reactivity due to VOCs (termed as VOCs reactivity) rather than VOCs mixing ratio was used in the calculation of ozone production rate (Geddes et al., 2009; LaFranchi et al., 2011; Sinha et al, 2012; Zhang et al., 2014). Due to the limitation of current measurement techniques, some VOCs species which could not be quantified so far, and therefore cannot be integrated into current chemical mechanisms of model run, could laid a great uncertainty in ozone production prediction. By directly measuring the total OH reactivity, VOCs reactivity can be obtained by deducting the inorganic reactivity from the total OH reactivity, which provides a constrain for evaluating the roles of reactive VOCs in air chemistry (Sadanaga et al, 2005; Sinha et al, 2012; Yang et al., 2016).

This paper presents field data in China from two intensive observation conducted in August 2013 in Beijing, and October to November 2014 in Heshan, Guangdong, focusing on OH reactivity and related species. The variations of total OH reactivity at both sites were compared with similar observations in urban and suburban areas worldwide. Thereafter, a zero dimensional box model based on Regional Atmospheric Chemical Mechanism 2 (RACM2) was employed for OH reactivity simulations. The possible missing reactivity and its importance for the ozone production calculation are discussed.

2. Methods

2.1 Total OH reactivity measurements

2.1.1 Measurement principles

Total OH reactivity was measured by the comparative reactivity method (CRM) first developed at Max Planck Institute for Chemistry (Sinha et al., 2008). The CRM system was built accordingly in Peking University, which consisted of 3 major components: inlet and calibration system, reactor, and measuring system as shown in

Fig 1. Ambient air was sampled after a teflon filter and then pumped through a 14.9m Teflon 3/8 inch (outer diameter) inlet at about 7 $L \cdot min^{-1}$ rate, with a 5 - 6 s residence time.

In this method, pyrrole (C_4H_5N) was used as the reference substance and was quantified by a quadrupole PTR-MS (Ionicon Analytic, Austria). There are 4 working modes for measuring procedure: In the C0 mode, pyrrole (Air Liquid Ltd, U.S.) is introduced into the reactor with dry synthetic air (99.99%, Chengweixin Gas Ltd, China). A mercury lamp (185nm, used for OH radicals generation) is turned off and high-pure dry nitrogen (99.99%, Chengweixin Gas Ltd, China), is mixed into the reactor through a second arm. In this mode, the highest signals of m/z 68 (protonated mass of pyrrole) c0 are obtained. Then in the C1 mode, the nitrogen and synthetic air is still dry but the mercury lamp is turned on. The mixing ratio of pyrrole decreased to c1. The difference between c0 and c1 is mainly due to the photolysis of pyrrole (Sinha et al., 2008). C2 mode is the "zero air" mode in which synthetic air and nitrogen are humidified before being introduced into the reactor. The photolysis of water vapor generates OH radicals which react with pyrrole in the reactor to c2 level. Then C3 mode is the measuring mode in which the automatic valve switches from synthetic air to ambient air. The ambient air is pumped into the reactor to react with OH radicals, competing with pyrrole molecules. The mixing ratio of pyrrole is detected as c3. Total OH reactivity is calculated as below, based on equations from Sinha et al. (2008):

$$k_{OH} = c1 \times k_{Pyr+OH} \times \frac{c3-c2}{c1-c3} \quad (2\text{-}1)$$

Ambient air or synthetic air was introduced at 160 -170 ml min^{-1} with the total flow 320 – 350 ml min^{-1}(The typical dilution factor was about 2-2.15 depending on the situation). The residence time of air inside the reactor was less than 30 s before they were pumped by the Teflon pump. The typical c1 mixing ratio for pyrrole in Beijing and Heshan measurements were about 60 ppbV and 55 ppbV, while the mixing ratios of OH radicals generated by mercury lamp were about 35 ppbV and 28 ppbV. The mixing ratios were quite consistent for either of the campaigns, respectively. Corrections about pseudo-first order kinetics were conducted for both

152 measurements, based on the methods in Sinha et al (2008). The typical correction
153 factors could be presented as

154 $$R_{true} = 0.0008 * (R_{mea})^2 + 0.78 * R_{mea} - 0.042 \quad (2\text{-}2)$$

155 $$R_{true} = -0.0004 * (R_{mea})^2 + 0.81 * R_{mea} - 0.017 \quad (2\text{-}3)$$

156 **2.1.2 Calibrations and tests**

157 We performed two calibrations for the measurements. First, PTR-MS was
158 calibrated by diluted dry pyrrole standard gas ranging from less than 10 ppbV to over
159 160 ppbV (presented in Fig S1). Additionally, we conducted an inter-comparison with
160 humidified pyrrole dilution gas. The sensitivity was about 3% to 5% higher than dry
161 calibration, which was considered for later calculation (Sinha et al., 2009). The tests
162 of the CRM system were done by using both the single standard gas, such as CO,
163 propane, propene (Huayuan Gas Ltd, China) and a standard of the mixture of 56
164 non-methane hydrocarbons (NMHCs) (SpecialGas Ltd, U.S.). The results of the
165 calibrations and tests were presented in Fig 2. Measured and calculated OH reactivity
166 agreed well within the uncertainty for all calibrations.

167 A key factor influencing the measurement results is the stability of OH radical
168 generator. One major interference could be the difference in relative humidity
169 between C2 mode and C3 mode. During the experiment, we used one single needle
170 valve to control the flow rate of synthetic air going through the bubbler, so that the
171 relative humidity during C2 mode could be adjusted to match humidity during
172 ambient sampling (C3 mode). Meanwhile, the remaining minor difference could be
173 corrected by factors derived from the OH reactivity-humidity correction experiment.
174 The details of the OH-correction experiment and the data were presented in the
175 supporting information (Fig. S1 and S2).

176 The other interference might be caused by ambient NO, which produces
177 additional OH radicals via recycling of HO_2 radicals (Sinha et al., 2008; Dolgorouky
178 et al., 2012; Michoud et al., 2015). The amount of OH radical through this pathway is
179 hard to be quantified. In the morning rush hours or on polluted cloudy days, NO
180 levels could rise to over 30 ppbV in both Beijing and Heshan, which could then
181 potentially introduce high uncertainties for measurements. The NO-correction

experiments were conducted by introducing given amounts of VOCs standard gases into the reactor. When the stable concentrations for c2 were reached, different levels of NO were injected into the reactor and the "measured" reactivity decreased as the NO mixing ratio increased. Then a correction curve was fitted between the differences in reactivity and NO mixing ratios. Several standard gases and different levels of base reactivity (from less than $30s^{-1}$ to over $180s^{-1}$) have been tried and the curve was quite consistent for all tested gases, as shown in Fig 3. The correction derived from the curve was used later to correct ambient measurements according to simultaneous detected NO levels. The correction was necessary when NO mixing ratio was larger than 5 ppbV, which was quite often observed in the morning time as well as cloudy days in Beijing and Heshan. The relative change for reactivity results could be over 100 s^{-1} when NO mixing ratio was about 30 ppbV.

A further potential interference comes from nitrous acid (HONO). The photolysis of HONO in the reactor could generate the same amount of OH radicals and NO molecules, as shown in R1. The additional OH radicals and NO molecules can be both interferences with the reactivity measurements. Similar correction experiments were conducted as the NO correction experiment. HONO were added stepwise in several mixing ratios (1-10 ppbV), generated by a HONO generator (Liu et al., 2016) and thus introduced into the reactor. A curve was fitted between the differences in reactivity and HONO mixing ratios, as presented in Fig 4. The correction associated with this curve was also applied later in the ambient measurements.

$$HONO \xrightarrow{h\gamma} OH+NO \qquad (R1)$$

To make sure the production of OH radicals was stable during the experiments, C1 mode was measured for 1-2 hour every other day and C2 mode was measured for 20-30 minutes every two hours. With above calibrations and tests into consideration, the detection limits of CRM methods in two campaigns was around 5 s^{-1} (2 σ). The total uncertainty of the method was about 20% (1 σ), due to rate coefficient of pyrrole reactions (15%), flow fluctuation (3%), instrument precision (6% when measured reactivity > 15 s^{-1}), standard gases (5%) and corrections for relative humidity (5%).

2.2 Field measurements

2.2.1 Measuring sites and periods

The urban measurements started from August 10th to August 27th, 2013 at Peking University (PKU) Site (116.18°E, 39.99°N), which was set on the roof of a 6-floor building. The site is about 300 m from the 6-lanes road to the east and 500 m to the 8 -lanes road to the south. This site is an urban site used for intensive field measurements of air quality in Beijing for long. Detailed information about this site can be found elsewhere (Yuan et al., 2012).

Suburban measurements were conducted from October 20th to November 22nd 2014 at Heshan (HS) site, Guangdong (112.93°E, 22.73°N). The site is located on top of a small hill (60 m above ground) in Jiangmen, which is 50km from a medium size city Foshan (with a population of about 7 million) and 80 km from a megacity Guangzhou. This is the super-site for measurements of air quality trends by Guangdong provincial government, detailed information about which can also be found in Fang et al (2016).

2.2.2 Simultaneous measurements

During both intensive campaigns, fundamental meteorological parameters and trace gases were measured simultaneously. Meteorological parameters, such as temperature, relative humidity, pressure, wind speed, wind direction were measured. NO and NO_x mixing ratios were measured by chemi-luminescence (model 42i, Thermo Fischer Inc, U.S.), and O_3 was measured by UV absorption (model 49i, Thermo Fischer Inc, U.S.). CO was measured by Gas Filter Correlation (model 48i, Thermo Fischer Inc, U.S.), and SO_2 was measured by pulsed fluorescence (model 43C, Thermo Fischer Inc, U.S.). The photolysis frequencies were measured by a spectral radiometer (SR) including 8 photolysis parameters. These parameters were all averaged into 1-minute resolution. The performances of these instruments were presented in Table S1 and Table S2.

VOCs were measured by a cryogen-free online GC-MSD/FID system, developed by Peking University (Yuan et al., 2012; Wang et al., 2014a). The time resolution is 1

hour but the sampling time starts from the 5th minute to 10th minute every hour. The system was calibrated by two sets of standard gases: 56 NMHCs including 28 alkanes, 13 alkenes and alkynes, 15 aromatics; EPA TO-15 standards (http://www.epa.gov/ttnamti1/les/ambient/airtox/to-15r.pdf), including additional OVOCs and halocarbons. The detection limits ranged from 10ppt-50ppt, depending on the species. Formaldehyde was measured by the Hantzsch method with time resolution of 1 minute. Detailed information about this instrument is described in one previous paper (Li et al., 2014).

2.3 Model description

2.3.1 Box model

A zero-dimensional box model was applied to produce the unmeasured secondary products and OH reactivity for both field observations. The chemical mechanism employed in the model was RACM2 (Stockwell et al., 1997, Goliff et al., 2013), with implementation of Mainz Isoprene Mechanism (MIM, Pöschl et al., 2000) and update versions by Geiger et al. (2003) and Karl et al. (2006) for isoprene reactions. The model was constrained by measured photolysis frequencies, ancillary meteorology and inorganic gases measurements, as well as VOCs data. Mixing ratios of methane and H_2 were set to be 1.8 ppmV and 550 ppbV. The model was calculated in a time-dependent mode with 5-min time resolution. Each model run started with 3 days spin-up time to reach steady-state conditions for long-lived species. Additional loss by dry deposition was assumed to have a corresponding lifetime of 24 hours to avoid the accumulation of secondary productions.

2.3.2 Ozone production efficiency

Ozone production efficiency (OPE) is defined as the number of molecules of total oxidants produced photochemically when a molecule of NO_x was oxidized (Kleinman, 2002, Chou et al., 2011). It helps to evaluate the impacts of VOCs reactivity on ozone production in various NO_x regimes. In this work, the OPE was expressed as the ratio of ozone production rate (i.e. $P(O_3)$) to NO_x consumption rate (i.e. $D(NO_x)$). NO_z, calculated as the difference between NO_y (sum of all odd-nitrogen compounds) and NO_x, was assumed to be the oxidation products of NOx. Thus the

OPE could be also calculated as $P(O_3)/P(NO_z)$. The ozone production rate is obtained as 2-2, and the $P(NO_z)$ is approximately as production rate of HNO_3 as well as the production rate of organic nitrate, which is given as 2-3.

$$P(O_3) = k_{HO_2+NO}[HO_2][NO] + \sum_i k_{RO_{2_i}+NO}[RO_{2_i}][NO] \quad (2\text{-}2)$$

$$P(NO_z) = k_{NO_2+OH}[NO_2][OH] + \sum_i k_{RO_i+NO_2}[RO_i][NO_2] \quad (2\text{-}3)$$

3. Results

3.1 Time series of meteorology and trace gases

The time series of selected meteorological parameters and inorganic trace gases were presented in 5 minute averages (Fig 5). The median values of the inorganic trace gases were 0.715 ± 0.335 ppmV for CO, 6.3 ± 5.75 ppbV for NO and 36.5 ± 21.3 ppbV for NO_2, 57 ± 44 ppbV for O_3 in Beijing. In Heshan, the median results were 0.635 ± 0.355 ppmV for CO, 9.7 ± 6.95 ppbV for NO, 29.6 ± 12.6 ppbV for NO_2, and 55.7 ± 34.9 ppbV for O_3. Both results were within the range of data from literatures (Zhang et al., 2008; Zheng et al., 2010; Zhang et al., 2014). However, daytime averaged O_3 mixing ratio in Beijing 2013 was a little lower than the medium results (about 60 ppbV) in normal years (Zhang et al., 2014). This could be due to higher frequencies of cloudy and rainy days, which accounted for about 1/3 of our measurement duration. The measured maximum photolysis rates in cloudy/rainy days were about half of peak values of J (O^1D) on sunny days. Even under this circumstances, ozone levels from the campaign remained high, the pollution episodes with ozone exceeding Grade II of China National Ambient Air Quality Standards (93 ppbV) occurred quite often, and the percentage of exceedance were 40% in Beijing and 20% in Heshan.

The mixing ratios of VOCs in both campaigns were presented in Table S3 and Table S4. In summer Beijing, alkanes accounted for over 60% of the summed VOCs mixing ratios during most of the time, while in Heshan the contribution from aromatics was 6% higher than that in Beijing. This could be explained by stronger emissions from solvent use and paint industry in the PRD region (Zheng et al., 2009). The ratio of toluene to benzene, which is typically used qualitatively as an indicator

for aromatics emission sources also supported this assumption. While this ratio in Beijing was close to 2, similar to vehicle emissions (Barletta et al., 2005), the ratio in Heshan was higher than 3 due to strict control of benzene in solvent usage these days (Barletta et al., 2005; Liu et al., 2008). In the ozone polluted episode in Fig 5, the mixing ratios of most species were about twice to three times higher than the daily average results.

The diurnal variations of NO_x, O_3 and photochemical age from Beijing and Heshan site were compared in Fig 6 and Fig 7. Both sites presented similar diurnal patterns for O_3 and NO. However, the highest 1-hour average O_3 value at PKU site came in the afternoon and stayed at high level till the dawn. While O_3 pattern at Heshan site did not stay high in the afternoon. An additional similarity was that the NO peaks occurred at similar times for both sites. But NO decreased at a slower rate in Heshan till even 12:00 p.m. This was likely explained by the facts that the NO observed at PKU site was mainly from local vehicle emissions while NO_x at Heshan site was significantly influenced by long-range transported of air masses.

VOCs measurements provided us chance to evaluate the oxidation state at two sites. Based on the OH exposure calculation methods (de Gouw et al., 2005), we chose a pair of VOCs species: m,p-xylene and ethylbenzene to calculate the photochemical age:

$$[\mathrm{OH}]\Delta t = [\ln(\frac{[E]}{[X]})_t - \ln(\frac{[E]}{[X]})_0]/(k_E - k_x) \quad (3\text{-}1)$$

Here, [E] and [X] represents the mixing ratios of ethylbenzene and m,p-xylene, k_E and k_X means the OH reaction rate coefficient of ethylbenzene and m,p-xylene. As presented in Fig 7, we chose 1.15 ppbV $ppbV^{-1}$ and 2.3 ppbV $ppbV^{-1}$ as emission ratios of ethylbenzene to m,p-xylene in Beijing and Heshan, as they were the largest ratios in diurnal variations for the campaign. The largest OH exposure in Beijing 2013 was calculated as 0.71×10^{11} molecule s cm^{-3} in 13:00 LTC, while the largest OH exposure in Heshan 2014 was calculated to be 1.69×10^{11} molecule s cm^{-3} in 14:00 LTC. The results in Beijing were comparable to previous reports (Yuan et al., 2012). Assuming the daytime average ambient OH concentration was 5.2×10^6 molecule

329 cm^{-3} (Lu et al., 2013), the photochemical age in Beijing was estimated to be not more
330 than 3.5 h. With measured daytime average OH concentration as 7.5×10^6 molecule
331 cm^{-3} in Heshan (Tan et al., in preparation), the photochemical age in Heshan was
332 about 6 h to 7 h, which was about twice the photochemical age of the Beijing
333 observations, indicating a more aged atmospheric environment in Heshan. However,
334 the assumed OH radical concentrations' influence on the photochemical age results
335 should not be neglected.

336 **3.2 Measured reactivity**

337 Total OH reactivity ranged from less than 10 s^{-1} to over 100 s^{-1} in Beijing (Fig
338 5a). The daily median value was 20 ± 11 s^{-1}. The diurnal patterns changed
339 significantly from day to day (Fig 8). The averaged diurnal pattern showed that the
340 total OH reactivity was higher from dawn to morning rush hours with a peak hourly
341 mean of 27 s^{-1}, and decreased to a lower value, median value of 17 s^{-1} in the afternoon.
342 This diurnal pattern was similar to the variations of NO_x mixing ratios (Williams et al.,
343 2016).

344 Meanwhile, measured total OH reactivity in Heshan was higher in median but
345 the diel variation was less evident. The daily median value was 31 ± 20 s^{-1}. The OH
346 reactivity was much less variable in the daily variation. This could possibly due to the
347 more aged air masses in Heshan, as presented in 3.1. The other probable explanation
348 could be the two periods of clean air we encountered, during which ground-level
349 ozone and $PM_{2.5}$ concentrations were rather low, each of the cases lasted for about 5
350 days during our measurements. And 2 pollution episodes were identified between
351 October 24^{th} to 27^{th} and November 14^{th} to 17^{th}, 2014. Both episodes showed
352 accumulation of ozone and $PM_{2.5}$. The total OH reactivity level also built up
353 significantly (Fig 5b).

354 **3.3 Variations in missing reactivity**

355 Significant differences were found between the measured reactivity and
356 calculated reactivity which derived from mixing ratios of different species multiplied
357 by their rate coefficients with OH radicals. Taking all measured species into
358 consideration, NO_x and NMHCs showed the largest contribution, 45%-55% of total

OH reactivity (Fig 9). The OVOCs had also significant contribution, and measured OVOCs had a sharing of 10% in total reactivity in Beijing while 7% in Heshan.

The Missing reactivity was on average over 4 s^{-1}, 21 ± 17 % of the total OH reactivity in Beijing and 10 s^{-1}, 32 ± 21% in Heshan. The missing reactivity presented different temporal patterns. In Beijing, the missing reactivities were high during pollution episodes, especially in the morning rush hours. The percentage of missing reactivity could reach over 50%. For the Heshan site, the missing reactivity was more or less stable during the entire campaign. Even in clean days with reactivity levels lower than 20 s^{-1}, 20%-30% of missing reactivity still existed.

4. Discussion

4.1 Reactivity levels in Beijing and Heshan

The measured VOCs reactivity (obtained by subtracting inorganic reactivity from total OH reactivity), 11.2 s^{-1} in Beijing and 18.3 s^{-1} in Heshan (Fig 10), was actually not at high end comparing with the levels from literatures. Tokyo presented a similar level of VOCs reactivity (Yoshino et al., 2006) and Paris had an even higher level of VOCs reactivity which was obtained in wintertime (Dolgorouky et al., 2012). The measured NMHCs levels (obtained by adding all hydrocarbon mixing ratios together) were also not very high, with Beijing 2013 being around 20 ppbV and Heshan 2014 higher than 35 ppbV. The relative VOCs reactivity, defined by the ratio of the VOCs reactivity to the measured NMHCs levels, the values for both Beijing and Heshan were very high.

One possible explanation is the higher content of reactive hydrocarbons in China. Compared to other campaigns, both sites had higher loading of alkenes and aromatics (Yuan et al., 2012; Wang et al., 2014b). The other probable reason is the contribution from OVOCs. In Beijing and Heshan, ambient formaldehyde could accumulate to over 10 ppbV, which was significantly higher than levels found in other observations (Li et al., 2013; Chen et al., 2014). Another possible explanation is unmeasured species, either primary hydrocarbons or secondary products, which will be discussed in later sessions.

388 **4.2 Contributions to the missing reactivity: primary VOCs**

389 As missing reactivity was observed at Beijing and Heshan site, the species
390 possibly causing these missing were examined. Throughout the whole campaign at the
391 PKU site, missing reactivity was normally found in the morning, as for an example in
392 August 16th and 17th 2013 in (Fig 11). Between 5 a.m. to 10 a.m., local vehicle-related
393 sources were strong, and the chemical reactions were not active yet, and the oxidants
394 levels thus the secondary VOC species remained low. We assumed that the
395 unmeasured primary VOCs species could most likely be the major contributors to
396 missing reactivity. Special attention was paid to the unmeasured branched-alkenes for
397 their high reactivity and was previously observed from vehicle exhaust (Nakashima et
398 al., 2010) and gasoline evaporation emissions (Wu et al., 2015). We found only one
399 dataset of branched alkenes measurements in 2005 measured by NOAA (Liu et al.,
400 2009). We chose the diurnal patterns of missing reactivity in Beijing in 2013 and
401 compared to the diel cycles of four measured branched-alkenes in 2005. The
402 correlations were found as presented in Fig 11. Considering the contribution of the 4
403 branched alkenes, the VOCs reactivity could be enhanced by 2.3 s^{-1}. This could only
404 partially explain the missing VOCs reactivity which was around 10 s^{-1}. With observed
405 decreasing trends in mixing ratios of most NMHCs species in Beijing (Zhang et al.,
406 2014; Wang et al., 2015), the branched-alkenes were insufficient to tell the full story
407 of the missing reactivity. Unmeasured semi-volatile organic compounds (SVOCs) and
408 intermediate volatile organic compounds (IVOCs), such as alkanes between C12 to
409 C30, and polycyclic aromatic hydrocarbons (PAHs) could be also important. Sheehy
410 (2010) found SVOCs and IVOCs contributed to about 10% in morning time in
411 Mexico City. Future studies with a wider range of reactive VOCs measurement for
412 total OH reactivity closure is needed.

413 **4.3 Contributions to the missing reactivity: secondary VOCs**

414 Due to limitations in chemistry mechanisms as well as measuring techniques,
415 secondary products are not fully quantified in ambient air and could probably
416 contribute significantly to the observed missing reactivity, especially in the urban or
417 suburban sites receiving chemically complex aged air masses.

Besides the large missing reactivity during the morning rush hour, there was about 25% difference between measured and calculated reactivity from August 16th to 18th, 2013 at PKU site. Considering high levels of oxidants in daytime, the mixing ratios of branched-alkenes could be lower than 0.1 ppbV, which could not explain the observed missing reactivity. A box model was deployed to investigate the role of secondary species in variation of VOCs reactivity. The model, constrained by measured parameters (meteorology, inorganic gases, VOCs including measured carbonyls), gave the results of VOCs reactivity which agreed well with the measured reactivity in most of the daytime (Fig 11). Major contributors from modeled species were unmeasured aldehydes, glyoxal and methyl glyoxal. Average values of major secondary contributors to modelled reactivity were provided in Table S5. However, the missing in morning hours remain unsolved: In the model run, the higher secondary contribution on August 17th 2013 morning was owing to isoprene oxidation products, by using 1.5 ppbv of isoprene levels as model input, the missing reactivity kept over 40% around 7:00 and 8:00 a. m.

The similar model was applied for the Heshan observation (Fig 12). During the polluted episode between October 24th and 27th 2014, a 30% missing reactivity existed for most time. Unfortunately, the modeled reactivity was only 10-20% higher than calculated reactivity, and not enough to explain the measured reactivity. The major contributors among modeled species were also unmeasured aldehydes, glyoxal, methyl glyoxal and other secondary products, as shown in Table S6. Due to strong emissions of aromatics from solvent use and petroleum industry in PRD region (Zheng et al., 2009), high levels of glyoxal and methyl glyoxal in this region were observed from satellite measurement (Liu et al., 2012) and ground measurements (Li et al., 2013). Compared to the 2006 measurements in Back garden, a semi-rural site in PRD region, the modeled glyoxal was twice as high as around 0.8 ppbV (Li et al., 2013). This difference possibly resulted from higher levels of precursors in 2014 measurements, where the measured reactivity was about 50% higher than the results in Backgarden 2006 (Lou et al., 2010).

4.4 Implications for ozone production efficiency

The investigating of missing in VOCs reactivity is expected to better understand the ozone formation processes. To evaluate this contribution, we employed the box model to calculate the influence of VOCs reactivity on OPE. We set two scenarios for the model run: 1) The base run was constrained with measured species, including all inorganic compounds, PAMS 56 hydrocarbons, TO-15 OVOCs and formaldehyde. This is how we obtained the modelled reactivity as presented above, and the intermediates and oxidation products were reproduced as well. 2) The other scenario used measured reactivity as a constraint. Due to the difference between measured and modeled reactivity, we allocated the missing reactivity into several groups. For the primary species, we assumed the ratio between total chain-alkenes and branched-alkenes were the same in Beijing 2013 and in Heshan 2014 as the ratio in Beijing 2005, so we got the assumed mixing ratios of branched-alkenes at both sites. For secondary species, we allocated the remaining missing reactivity into different intermediates or products based on weights obtained in the model base run. Under both assumptions, we ran the OBM and calculated the OPE, as presented in Fig 13.

For both sites, the OPE constrained by measured reactivity were significantly higher than the OPE we calculated from modeled reactivity. In Beijing, the OPE from measured reactivity was about 21% higher on average. The value was 30% higher at Heshan site under similar assumptions. This percentage was close to the percentage of missing reactivity, indicating the ignorance of unmeasured or unknown organic species can cause significant underestimation in ozone production calculation.

Compared to other similar calculations worldwide, the OPE results for Beijing and Heshan were significantly higher (Fig 14). The comparison was made for NO_x = 20 ppbV which was in the range of most observation results. For urban measurements, only the results from Mexico City in MCMA-03 were close to the Beijing results in basic model run (Lei et al., 2008). For suburban measurements, the OPE in Heshan 2014 was higher than all other three campaigns, even including the results from Shangdianzi station in CAREBEIJING-2008 campaigns (Ge et al., 2012). While taking missing reactivity into consideration, the OPE results were even higher, indicating more ozone was produced by the reactions of the same quantity of NO_x

478 molecules.

479 5. Conclusions

480 In this study, total OH reactivity measurements employing CRM system were
481 conducted at PKU site in Beijing 2013, and Heshan site 2014 in PRD region.
482 Comparisons between measured and calculated, as well as modelled reactivity were
483 made and possible reasons for the missing reactivity have been investigated. The
484 contribution of missing reactivity to ozone production efficiency was evaluated.

485 In Beijing 2013, daily median result for measured total OH reactivity was 20 ±
486 11 s^{-1}. Similar diurnal variation with other urban measurements was found with peaks
487 over 25 s^{-1} during the morning rush hour and lower reactivity than 16 s^{-1} in the
488 afternoon. In Heshan 2014, total OH reactivity was 31 ± 20 s^{-1} on daily median result.
489 The diurnal variation was not significant. Both sites have experienced OH reactivity
490 over 80 s^{-1} during polluted episodes.

491 Missing reactivity was found at both sites. While in Beijing the missing
492 reactivity made up 21% of measured reactivity, some periods even reached a higher
493 missing percentage as 40%-50%. In Heshan, missing reactivity's contribution to total
494 OH reactivity was 32% on average and quite stable for the whole day. Unmeasured
495 primary species, such as branched-alkenes could be important contributor to the
496 missing reactivity in Beijing, especially in morning rush hour, but they were not
497 enough to explain Aug 17th morning's event. With the help of RACM2, unmeasured
498 secondary products were calculated and thus the modelled reactivity could agree with
499 measured reactivity in Beijing in the noontime. However, they were still not enough
500 to explain the missing reactivity in Heshan, even in daytime. This was probably
501 because of the relatively higher oxidation stage in Heshan than in Beijing.

502 Missing reactivity could impact the estimation of atmospheric ozone production
503 efficiency. Compared to modeled reactivity from base run, ozone production
504 efficiency would rise 21% and 30% in Beijing and Heshan with measured reactivity
505 applied. Both results were significantly higher than similar observations worldwide,
506 indicating the relatively faster ozone production at both sites.

However, in order to further explore the OH reactivity in both regions, more efforts should be paid in both OH reactivity measurements and speciated measurements, as well as modeling to close the total OH reactivity budget. Moreover, a thorough way with more detailed mechanisms should be established to connect the missing reactivity to the evaluation of ozone production.

Acknowledgement

This study was funded by the National Key Research and Development Plan (grant no. 2016YFC020200), Natural Science Foundation for Outstanding Young Scholars (grant no. 41125018) and a Natural Science Foundation key project (grant no.411330635). The research was also supported by the European Commission Partnership with China on Space Data (PANDA project). Special thanks to Jing Zheng, Mei Li, Yuhan Liu from Peking University and Tao Zhang from Guangdong Environmental Monitoring Center for the help, thanks for William. C. Kuster from NOAA . Earth System Research Laboratory for the branched-alkenes data in 2005.

Reference

Barletta, B., Meinardi, S., Sherwood Rowland, F., Chan, C.-Y., Wang, X., Zou, S., Yin Chan, L., and Blake, D. R.: Volatile organic compounds in 43 Chinese cities, Atmos. Environ., 39, 5979-5990, doi: 10.1016/j.atmosenv.2005.06.029, 2005.

Calpini, B., Jeanneret, F., Bourqui, M., Clappier, A., Vajtai, R., and van den Bergh, H.: Direct measurement of the total reaction rate of OH in the atmosphere, Analusis, 27, 328-336, doi: 10.1051/analusis:1999270328, 1999.

Chatani, S., Shimo, N., Matsunaga, S., Kajii, Y., Kato, S., Nakashima, Y., Miyazaki, K., Ishii, K., and H., U.: Sensitivity analyses of OH missing sinks over Tokyo metropolitan area in the summer of 2007, Atmos. Chem. Phys., 9, 8975-8986, doi:

10.5194/acp-9-8975-2009, 2009.
Chen, W. T., Shao, M., Lu, S. H., Wang, M., Zeng, L. M., Yuan, B., Liu, Y.: Understanding primary and secondary sources of ambient carbonyl compounds in Beijing using the PMF model. Atmos. Chem. Phys., 14, 3047-3062, doi: 10.5194/acp-14-3047-2014, 2014.
Chou, C. C. K., Tsai, C. Y., Chang, C. C., Lin, P. H., Liu, S. C., and Zhu, T.: Photochemical production of ozone in Beijing during the 2008 Olympic Games, Atmos. Chem. Phys., 11, 9825-9837, doi: 10.5194/acp-11-9825-2011, 2011.
Dodge, M. C.: Proceedings of the international conference on photochemical oxidant pollution and its control. Combined use of modeling techniques and smog chamber data to derive ozone-precursor relationships, U.S. Environmental Protection Agency, Research Triangle Park, NC, 881-889 pp., 1977.
de Gouw, J. A., Middlebrook, A. M., Warneke, C., Goldan, P. D., Kuster, W. C., Roberts, J. M., Fehsenfeld, F. C., Worsnop, D. R., Canagaratna, M. R., Pszenny, A. A. P., Keene, W. C., Marchewka, M., Bertman, S. B., Bates, T. S.: Budget of organic carbon in a polluted atmosphere: Results from the New England Air Quality Study in 2002, J. Geophy. Res.-Atmos., 110, D16305, doi: 10.1029/2004jd005623, 2005.
Dolgorouky, C., Gros, V., Sarda-Esteve, R., Sinha, V., Williams, J., Marchand, N., Sauvage, S., Poulain, L., Sciare, J., and Bonsang, B.: Total OH reactivity measurements in Paris during the 2010 MEGAPOLI winter campaign, Atmos. Chem. Phys., 12, 9593-9612, doi: 10.5194/acp-12-9593-2012, 2012.
Edwards, P. M., Evans, M. J., Furneaux, K. L., Hopkins, J., Ingham, T., Jones, C., Lee, J. D., Lewis, A. C., Moller, S. J., Stone, D., Whalley, L. K., and Heard, D. E.: OH reactivity in a South East Asian tropical rainforest during the Oxidant and Particle Photochemical Processes (OP3) project, Atmos. Chem. Phys., 13, 9497-9514, doi: 10.5194/acp-13-9497-2013, 2013.
Fang, X., Shao, M., Stohl, A., Zhang, Q., Zheng, J., Guo, H., Wang, C., Wang, M., Ou, J., Thompson, R. L., and Prinn, R. G.: Top-down estimates of benzene and toluene emissions in the Pearl River Delta and Hong Kong, China, Atmos. Chem. Phys., 16, 3369-3382, doi: 10.5194/acp-16-3369-2016, 2016.
Fuchs, H., Hofzumahaus, A., Rohrer, F., Bohn, B., Brauers, T., Dorn, H. P., Häseler, R., Holland, F., Kaminski, M., Li, X., Lu, K., Nehr, S., Tillmann, R., Wegener, R., and Wahner, A.: Experimental evidence for efficient hydroxyl radical regeneration in isoprene oxidation, Nature Geoscience, 6, 1023-1026, doi: 10.1038/ngeo1964, 2013.

571 Fuchs, H., Tan, Z. F., Lu, K. D., Bohn, B., Broch, B., Brown, S. S., Dong, H. B.,
572 Gomm. S., Haseler, H. L. Y., Hofzumahaus, A., Holland, F., Li, X., Liu, Y., Lu, S. H.,
573 Min, K.-E., Rohrer, F., Shao, M., Wang, B. L., Wang, M., Wu, Y. S., Zeng, L. M.,
574 Zhang, Y. S., Wahner, A., Zhang, Y. H.: OH reactivity at a rural site (Wangdu) in the
575 North China Plain: Contributions from OH reactants and experimental OH budget,
576 Atmos. Chem. Phys., Dis., 716-745, doi: 10.5194/acp-2016-716, 2016.
577 Ge. B. Z., Sun. Y. L., Liu. Y., Dong. H. B., Ji. D. S., Jiang. Q., Li. J., Wang. Z. F.:
578 Nitrogen dioxide measurement by cavity attenuated phase shift spectroscopy (CAPS)
579 and implications in ozone production efficiency and nitrate formation in Beijing,
580 China. J. Geophy. Res.-Atmos., 118, 9499-9509, doi: 10.1002/jgrd.50757, 2013.
581 Geddes, J. A., Murphy, J. G., and K., W. D.: Long term changes in nitrogen oxides and
582 volatile organic compounds in Toronto and the challenges facing local ozone control,
583 Atmos. Environ., 43, 3407-3415, doi: 10.1016/j.atmosenv.2009.03.053, 2009.
584 Geiger, H., Barnes, I., Bejan, I., Benter, T., and Spittler, M.: The tropospheric
585 degradation of isoprene: an updated module for the regional atmospheric chemistry
586 mechanism, Atmos. Environ., 37, 1503–1519, doi: 10.1016/S1352-2310(02)01047-6,
587 2003.
588 Goliff, W. S., Stockwell, W. R., Lawson, C. V.: The regional atmospheric chemistry
589 mechanism, version 2. Atmos. Environ., 68, 174-185, doi:
590 10.1016/j.atmosenv.2012.11. 038, 2013
591 Hansen, R. F., Blocquet, M., Schoemaecker, C., Léonardis, T., Locoge, N., Fittschen,
592 C., Hanoune, B., Stevens, P. S., Sinha, V., and Dusanter, S.: Intercomparison of the
593 comparative reactivity method (CRM) and pump–probe technique for measuring total
594 OH reactivity in an urban environment, Atmos. Meas. Tech., 8, 4243-4264, doi:
595 10.5194/amt-8-4243-2015, 2015.
596 Ingham, T., Goddard, A., Whalley, L. K., Furneaux, K. L., Edwards, P. M., Seals, C. P.,
597 Self, D. E., Johnson, G. P., Read, K. A., Lee, J. D., and E., H. D.: a flow tube based
598 LIF instrument to measure OH reactivity in the troposphere, Atmos. Meas. Tech., 2,
599 465-477, doi: 10.5194/amt-2-465-2009, 2009.
600 Karl, M., Dorn, H.-P., Holland, F., Koppmann, R., Poppe, D., Rupp, L., Schaub, A.,
601 and Wahner, A.: Product study of the reaction of OH radicals with isoprene in the
602 atmosphere simulation chamber SAPHIR, J. Atmos. Chem., 55, 167–187, doi:
603 10.1007/s10874-006-9034-x, 2006.
604 Kato, S, Sato, T., Kaji, Y.: A method to estimate the contribution of unidentified VOCs

to OH reactivity. Atmos. Environ., 45, 5531-5539, doi: 10.1016/j.atmosenv.2011.05.074. 2011.

Kleinman, L. I., Daum, P. H., Imre, D. G., Lee. J. H., Lee. Y. N., Nunnermacker, L. J., Springston, S. R., Weinstein-Lloyd, J., Newman, L.: Ozone production in the New York City urban plume. J. Geophy. Res.-Atmos., 105, D11, 14495-14511, doi: 10.1029/2000 jd900011, 2000.

Kleinman, L. I.: Ozone production efficiency in an urban area, J. Geophy. Res. – atmos., 107, D23, 4733, doi: 10.1029/2002jd002529, 2002.

Kovacs, T. A., and Brune, W. H.: Total OH loss rate measurement, J. Atmos. Chem., 39, 105-122, doi: 10.1023/a:1010614113786, 2001.

Kovacs, T. A., Brune, W. H., Harder, H., Martinez, M., Simpas, J. B., Frost, G. J., Williams, A. G., Jobson, B. T., Stroud, C., Young, V., Fried, A., and B., W.: Direct measurements of urban OH reactivity during Nashville SOS in summer 1999, J. Environ. Monit., 5, 68-74, doi: 10.1039/b204339d, 2003.

Kumar V., Sinha, V.: VOC-OHM: a new technique for rapid measurements of ambient total OH reactivity and volatile organic compounds using a single proton transfer reaction mass spectrometer. Int. J. of Mass Spectrom., 374, 55-63. 2014.

LaFranchi, B. W., Goldstein, A. H., and Cohen, R. C.: Observations of the temperature dependent response of ozone to NO_x reductions in the Sacramento, CA urban plume, Atmos. Chem. Phys., 11, 6945-6960, doi: 10.5194/acp-11-6945-2011, 2011.

Lee, J. D., Young, J. C., Read, K. A., Hamilton, J. F., Hopkins, J. R., Lewis, A. C., Bandy, B. J., Davey, J., Edwards, P. M., Ingham, T., Self, D. E., Smith, S. C., Pilling, M. J., and Heard, D. E.: Measurement and calculation of OH reactivity at a United Kingdom coastal site, J. Atmos. Chem., 64, 53-76, doi: 10.1007/s10874-010-9171-0, 2010.

Lei, W., Zavala, M., Foy, B. de., Volkamer, R., Molina, L. T.: Characterizing ozone production and response under different meteorological conditions in Mexico City. Atmos. Chem. Phys., 8, 7571-7581, doi: 10.5194/acp-8-7571-2008, 2008.

Li, M., Shao, M., Li, L.-Y., Lu, S.-H., Chen, W.-T., and Wang, C.: Quantifying the ambient formaldehyde sources utilizing tracers, Chinese. Chem. Lett., 25, 1489-1491, doi: 10.1016/j.cclet.2014.07.001, 2014.

Li, X., Brauers, T., Hofzumahaus, A., Lu, K., Li, Y. P., Shao, M., Wagner, T., and Wahner, A.: MAX-DOAS measurements of NO_2, HCHO and CHOCHO at a rural site

639 in Southern China, Atmos. Chem. Phys., 13, 2133-2151, doi:
640 10.5194/acp-13-2133-2013, 2013.
641 Liu, Y., Shao, M., Fu, L., Lu, S., Zeng, L., and Tang, D.: Source profiles of volatile
642 organic compounds (VOCs) measured in China: Part I, Atmos. Environ., 42,
643 6247-6260, doi: 10.1016/j.atmosenv.2008.01.070, 2008.
644 Liu, Y., Shao, M., Kuster, W. C., Goldan, P. D., Li, X. H., Lu, S. H., de Gouw, J. A.:
645 Source identification of reactive hydrocarbons and oxygenated VOCs in the
646 summertime in Beijing. Environ. Sci. Technol., 43, 75-81, doi: 10.1021/es801716n,
647 2009.
648 Liu, Y. H., Lu, K. D., Dong, H. B., Li, X., Cheng, P., Zou, Q., Wu, Y. S., Liu, X. G.,
649 Zhang, Y. H. In situ monitoring of atmospheric nitrous acid based on multi-pumping
650 flow system and liquid waveguide capillary cell. J. Envion. Sci. Accepted. 2016.
651 Liu, Z., Wang, Y., Vrekoussis, M., Richter, A., Wittrock, F., Burrows, J. P., Shao, M.,
652 Chang, C.-C., Liu, S.-C., Wang, H., and Chen, C.: Exploring the missing source of
653 glyoxal (CHOCHO) over China, Geophy. Res. Lett., 39, L10812, doi:
654 10.1029/2012gl051645, 2012.
655 Lou, S., Holland, F., Rohrer, F., Lu, K., Bohn, B., Brauers, T., Chang, C. C., Fuchs, H.,
656 Häseler, R., Kita, K., Kondo, Y., Li, X., Shao, M., Zeng, L., Wahner, A., Zhang, Y.,
657 Wang, W., and Hofzumahaus, A.: Atmospheric OH reactivities in the Pearl River
658 Delta – China in summer 2006: measurement and model results, Atmos. Chem. Phys.,
659 10, 11243-11260, doi: 10.5194/acp-10-11243-2010, 2010.
660 Lu, K. D., Zhang, Y. H., Su, H., Brauers, T., Chou, C. C., Hofzumahaus, A., Liu, S. C.,
661 Kita, K., Kondo, Y., Shao, M., Wahner, A., Wang, J. L., Wang, X., and T., Z.: Oxidant
662 (O_3+ NO_2) production processes and formation regimes in Beijing, J. Geophys.
663 Res.-Atmos., 115, D07303, doi: 10.1029/2009jd012714, 2010.
664 Lu, K. D., Hofzumahaus, A., Holland, F., Bohn, B., Brauers, T., Fuchs, H., Hu, M.,
665 Häseler, R., Kita, K., Kondo, Y., Li, X., Lou, S. R., Oebel, A., Shao, M., Zeng, L. M.,
666 Wahner, A., Zhu, T., Zhang, Y. H., and Rohrer, F.: Missing OH source in a suburban
667 environment near Beijing: observed and modelled OH and HO_2 concentrations in
668 summer 2006, Atmos. Chem. Phys., 13, 1057-1080, doi: 10.5194/acp-13-1057-2013,
669 2013.
670 Mao, J. Q., Ren, X. R., Chen, S., Brune, W. H., Chen, Z., Martinez, M., Harder, H.,
671 Lefer, B., Rappengluck, B., Flynn, J., and M., L.: Atmospheric oxidation capacity in
672 the summer of Houston 2006: Comparison with summer measurements in other

673 metropolitan studies, Atmos. Environ., 44, 4107-4115, doi: 10.1016/j.atmosenv.2009.
674 01.013, 2010.
675 Michoud, V., Hansen, R. F., Locoge, N., Stevens, P. S., and Dusanter, S.: Detailed
676 characterizations of the new Mines Douai comparative reactivity method instrument
677 via laboratory experiments and modeling, Atmos. Meas. Tech., 8, 3537-3553, doi:
678 10.5194/amt-8-3537-2015, 2015.
679 Nölscher, A. C., Williams, J., Sinha, V., Custer, T., Song, W., Johnson, A. M., Axinte,
680 R., Bozem, H., Fischer, H., Pouvesle, N., Phillips, G., Crowley, J. N., Rantala, P.,
681 Rinne, J., Kulmala, M., Gonzales, D., Valverde-Canossa, J., Vogel, A., Hoffmann, T.,
682 Ouwersloot, H. G., Vilà-Guerau de Arellano, J., and Lelieveld, J.: Summertime total
683 OH reactivity measurements from boreal forest during HUMPPA-COPEC 2010,
684 Atmos. Chem. Phys., 12, 8257-8270, doi: 10.5194/acp-12-8257-2012, 2012.
685 Nölscher, A. C., Yanez-Serrano, A. M., Wolff, S., de Araujo, A. C., Lavric, J. V.,
686 Kesselmeier, J., and Williams, J.: Unexpected seasonality in quantity and composition
687 of Amazon rainforest air reactivity, Nature communications, 7, 10383-10394, doi:
688 10.1038/ncomms10383, 2016.
689 Nakashima, Y., Kamei, N., Kobayashi, S., and Y., K.: Total OH reactivity and VOC
690 analyses for gasoline vehicular exhaust with a chassis dynamometer, Atmos. Environ.,
691 44, 468-475, doi: 10.1016/j.atmosenv.2009.11.006, 2010.
692 Pöschl, U., von Kuhlmann, R., Poisson, N., and Crutzen, P. J.: Development and
693 intercomparison of condensed isoprene oxidation mechanisms for global atmospheric
694 modeling, J. Atmos. Chem., 37, 29–52, doi: 10.1023/A:1006391009798, 2000.
695 Ren, X. R., Harder, H., Martinez, M., Lesher, R. L., Oliger, A., Shirley, T., Adams, J.,
696 Simpas, J. B., and H., B. W.: HO_x concentrations and OH reactivity observations in
697 New York City during PMTACS-NY2001, Atmos. Environ., 37, 3627-3637, doi:
698 10.1016/s1352-2310(03)00460-6, 2003.
699 Ren, X. R., Brune, W. H., Cantrell, C., Edwards, G. D., Shirley, T., Metcalf, A. R., and
700 L., L. R.: Hydroxyl and Peroxy Radical Chemistry in a Rural Area of Central
701 Pennsylvania: Observations and Model Comparisons, J. Atmos. Chem., 52, 231-257,
702 doi: 10.1007/s10874-005-3651-7, 2005.
703 Ren, X. R., Brune, W. H., Mao, J. Q., Mitchell, M. J., Lesher, R. L., Simpas, J. B.,
704 Metcalf, A. R., Schwab, J. J., Cai, C., and Y., L.: Behavior of OH and HO_2 in the
705 winter atmosphere in New York City, Atmos. Environ. 40, 252-263, doi:
706 10.1016/j.atmosenv. 2005.11.073, 2006a.

Ren, X. R., Brune, W. H., Oliger, A., Metcalf, A. R., Simpas, J. B., Shirley, T., Schwab, J. J., Bai, C., Roychowdhury, U., Li, Y., Cai, C., Demerjian, K. L., He, Y., Zhou, X. H., Gao, H., and J., H.: OH, HO_2, and OH reactivity during the PMTACS–NY Whiteface Mountain 2002 campaign: Observations and model comparison, J. Geophys. Res.-Atmos., 111, doi: 10.1029/2005jd006126, 2006b.

Sadanaga, Y., Yoshino, A., Kato, S., Yoshioka, A., Watanabe, K., Miyakawa, T., Hayashi, I., Ichikawa, M., Matsumoto, J., Nishiyama, A., Akiyama, N., Kanaya, Y., and Y., K.: The importance of NO_2 and volatile organic compounds in the urban air from the viewpoint of the OH reactivity, Geophy. Res. Lett., 31, L08102, doi: 10.1029/2004gl019661, 2004.

Sadanaga, Y., Yoshino, A., Kato, S., and Y., K.: measurements of OH reactivity and photochemical ozone production in the urban atmosphre, Environ. Sci. Technol., 39, 8847-8852, doi: 10.1021/es049457p, 2005.

Sheehy, P. M., Volkamer, R., Molina, L. T., and Molina, M. J.: Oxidative capacity of the Mexico City atmosphere – Part 2: A RO_x radical cycling perspective, Atmos. Chem. Phys., 10, 6993-7008, doi: 10.5194/acp-10-6993-2010, 2010.

Shirley, T. R., Brune, W. H., Ren, X. R., Mao, J. Q., Lesher, R., Cardenas, B., Volkamer, R., Molina, L. T., Molina, M. J., Lamb, B., Velasco, E., Jobson, T., and M., A.: Atmospheric oxidation in the MCMA during April 2003, Atmos. Chem. Phys., 6, 2753-2765, doi: 10.5194/acp-6-2753-2006, 2006.

Sinha, V., Williams, J., Crowley, J. N., and J., L.: The Comparative Reactivity Method - a new tool to measure total OH reactivity in ambient air, Atmos. Chem. Phys., 8, 2213-2227, doi: 10.5194/acp-8-2213-2008, 2008.

Sinha, V., Custer, T. G., Kluepfel, T., and Williams, J.: The effect of relative humidity on the detection of pyrrole by PTR-MS for OH reactivity measurements, Int. J. Mass Spectrom., 282, 108-111, doi: 10.1016/j.ijms.2009.02.019, 2009.

Sinha, V., Williams, J., Lelieveld, J., Ruuskanen, T. M., Kalos, M. K., Patokoski, L., Hellen, H., Hakola, H., Mogensen, D., Boy, M., Rinne, L., and M., K.: OH reactivity measurements within a boreal forest - evidence for unknown reactive emissions, Environ. Sci. Technol., 44, 6614-6620, doi: 10.1021/es101780b, 2010.

Sinha, V., Williams, J., Diesch, J. M., Drewnick, F., Martinez, M., Harder, H., Regelin, E., Kubistin, D., Bozem, H., Hosaynali-Beygi, Z., Fischer, H., Andrés-Hernández, M. D., Kartal, D., Adame, J. A., and Lelieveld, J.: Constraints on instantaneous ozone production rates and regimes during DOMINO derived using in-situ OH reactivity

741 measurements, Atmos. Chem. Phys., 12, 7269-7283, doi: 10.5194/acp-12-7269-2012,
742 2012.
743 Stockwell, W. R., Kirchner, F., Kuhn, M., and Seefeld, S.: A new mechanism for
744 regional atmospheric chemistry modeling, J. Geophys. Res.-Atmos., 102, D22,
745 25847-25879, doi: 10.1029/97jd00849, 1997.
746 Stone, D., Whalley, L. K., and Heard, D. E.: Tropospheric OH and HO_2 radicals: field
747 measurements and model comparisons, Chem. Soc. Rev., 41, 6348-6404, doi:
748 10.1039/c2cs35140d, 2012.
749 Tan, Z. F., Fuchs, H., Zhang, Y. H., et al., Atmos. Chem. Phys., in preparation.
750 Wang, M., Zeng, L., Lu, S., Shao, M., Liu, X., Yu, X., Chen, W., Yuan, B., Zhang, Q.,
751 Hu, M., and Zhang, Z.: Development and validation of a cryogen-free automatic gas
752 chromatograph system (GC-MS/FID) for online measurements of volatile organic
753 compounds, Anal. Methods, 6, 9424-9434, doi: 10.1039/c4ay01855a, 2014a.
754 Wang, M., Shao, M., Chen, W. T., Yuan, B., Lu, S. H., Zhang, Q., Zeng, L. M., Wang,
755 Q.: A temporally and spatially resolved validation of emission inventories by
756 measurements of ambient volatile organic compounds in Beijing, China. Atmos.
757 Chem. Phys. 14, 5871-5891, doi: 10.5194/acp-14-5871-2014, 2014b.
758 Wang, M., Shao, M., Chen, W., Lu, S., Liu, Y., Yuan, B., Zhang, Q., Zhang, Q., Chang,
759 C. C., Wang, B., Zeng, L., Hu, M., Yang, Y., and Li, Y.: Trends of non-methane
760 hydrocarbons (NMHC) emissions in Beijing during 2002–2013, Atmos. Chem. Phys.,
761 15, 1489-1502, doi: 10.5194/acp-15-1489-2015, 2015.
762 Wang, T., Ding, A., Gao, J., and Wu, W. S.: Strong ozone production in urban plumes
763 from Beijing, China. Geophy. Res. Lett., 33, L21806, doi: 10.1029/2006gl027689,
764 2006.
765 Whalley, L. K., Stone, D., Bandy, B., Dunmore, R., Hamilton, J. F., Hopkins, J., Lee, J.
766 D., Lewis, A. C., and Heard, D. E.: Atmospheric OH reactivity in central London:
767 observations, model predictions and estimates of in situ ozone production, Atmos.
768 Chem. Phys., 16, 2109-2122, doi: 10.5194/acp-16-2109-2016, 2016.
769 Williams, J.: Provoking the air, Environ. Chem., 5, 317-319, doi:10.1071/en08048,
770 2008.
771 Williams, J., and Brune, W. H.: A roadmap for OH reactivity research, Atmos.
772 Environ., 106, 371-372, doi: 10.1016/j.atmosenv.2015.02.017, 2015.
773 Williams, J., Keßel, S. U., Nölscher, A. C., Yang, Y. D., Lee, Y. N., Yáñez-Serrano, A.
774 M., Wolff, S., Kesselmeier, J., Klüpfel, T., Lelieveld, J., and Shao, M.: Opposite OH

775 reactivity and ozone cycles in the Amazon rainforest and megacity Beijing:
776 Subversion of biospheric oxidant control by anthropogenic emissions, Atmos.
777 Environ., 125, 112-118, doi: 10.1016/j.atmosenv.2015.11.007, 2016.
778 Wu, Y., Yang, Y. D., Shao, M., and Lu, S. H.: Missing in total OH reactivity of VOCs
779 from gasoline evaporation, Chinese. Chem. Lett., 26, 1246-1248, doi:
780 10.1016/j.cclet.2015.05.047, 2015.
781 Yang, Y., Shao, M., Wang, X., Nölscher, A. C., Kessel, S., Guenther, A., and Williams,
782 J.: Towards a quantitative understanding of total OH reactivity: A review, Atmos.
783 Environ.,134, 147-161, doi: 10.1016/j.atmosenv.2016.03.010, 2016.
784 Yoshino, A., Sadanaga, Y., Watanabe, K., Kato, S., Miyakawa, Y., Matsumoto, J., and
785 Y., K.: Measurement of total OH reactivity by laser-induced pump and probe
786 technique—comprehensive observations in the urban atmosphere of Tokyo, Atmos.
787 Environ., 40, 7869-7881, doi: 10.1016/j.atmosenv.2006.07.023, 2006.
788 Yoshino, A., Nakashima, Y., Miyazaki, K., Kato, S., Suthawaree, J., Shimo, N.,
789 Matsunaga, S., Chatani, S., Apel, E., Greenberg, J., Guenther, A., Ueno, H., Sasaki, H.,
790 Hoshi, J., Yokota, H., Ishii, K., and Kajii, Y.: Air quality diagnosis from
791 comprehensive observations of total OH reactivity and reactive trace species in urban
792 central Tokyo, Atmos. Environ., 49, 51-59, doi: 10.1016/j.atmosenv.2011.12.029,
793 2012.
794 Yuan, B., Shao, M., de Gouw, J., Parrish, D. D., Lu, S., Wang, M., Zeng, L., Zhang,
795 Q., Song, Y., Zhang, J., and Hu, M.: Volatile organic compounds (VOCs) in urban air:
796 How chemistry affects the interpretation of positive matrix factorization (PMF)
797 analysis, J. Geophys. Res.-Atmos., 117, D24302, doi: 10.1029/2012jd018236, 2012.
798 Zhang, Q., Yuan, B., Shao, M., Wang, X., Lu, S., Lu, K., Wang, M., Chen, L., Chang,
799 C. C., and Liu, S. C.: Variations of ground-level O_3 and its precursors in Beijing in
800 summertime between 2005 and 2011, Atmos. Chem. Phys., 14, 6089-6101, doi:
801 10.5194/acp-14-6089-2014, 2014.
802 Zhang, Y. H., Su, H., Zhong, L. J., Cheng, Y. F., Zeng, L. M., Wang, X. S., Xiang, Y.
803 R., Wang, J. L., Gao, D. F., and Shao, M.: Regional ozone pollution and
804 observation-based approach for analyzing ozone–precursor relationship during the
805 PRIDE-PRD2004 campaign, Atmos. Environ., 42, 6203-6218, doi:
806 10.1016/j.atmosenv.2008. 05.002, 2008.
807 Zhao, C., Wang, Y. H., Zeng, T.,: East China Plains: a "Basin" of ozone pollution,
808 Environ. Sci. Technol., 43, 1911-1915, doi: 10.1021/es8027764, 2009.

Zheng, J. Y., Shao, M., Che, W. W., Zhang, L. J., Zhong, L. J., Zhang, Y. H., Streets, D., Speciated VOC emission inventory and spatial patterns of ozone formation potential in the Pearl River Delta, China. Environ. Sci. Technol. 43, 8580–8586, doi: 10.1021/es901688e, 2009.

Zheng, J. Y., Zhong, L. J., Wang, T., Louie, P. K. K., Li, Z. C.: Ground-level ozone in the Pearl River Delta region: analysis of data from a recently established regional air quality monitoring network. Atmos. Environ. 44, 814-823, doi: 10,1016/j/atmosenv. 2009.11.032, 2010.

Zhao. W., Cohan, D. S., Henderson. B. H.: Slower ozone production in Houston, Texas following emission reductions: evidence from Texas Air Quality Studies in 2000 and 2006. Atmos. Chem. Phys. 14, 2777-2788, doi: 10.5194/acp-14-2777-2014, 2014.

830 Table 1 Total OH reactivity measurements in urban areas

Campaign	Site	Year	method	$k_{OH(measured)}$ (s^{-1}) [a]	$k_{OH\ (calculated)}$ (s^{-1} if it is a value) [b]	Measured species [c]	Reference
SOS	Nashville, US	summer, 1999	LIF-flow tube	11.3	7.2	SFO	Kovacs et al., 2001; 2003;
PMTACS-NY 2001	NY, US	summer, 2001	LIF-flow tube	15~25	within 10%	SFO	Ren et al., 2003
PMTACS-NY 2004	NY, US	winter, 2004	LIF-flow tube	18-35	statistically lower	SF	Ren et al., 2006a
MCMA-2003	Mexico City, Mexico	spring, 2003	LIF-flow tube	10~120	30% less than	-[d]	Shirley et al., 2006
TexAQS	Houston, US	summer, 2000	LIF-flow tube	7~12	agree well	SFO	Mao et al., 2010
TRAMP2006	Houston, US	summer, 2006	LIF-flow tube	9-22	agree well	SFOB	Mao et al., 2010
	Tokyo, Japan	2003-2004	LP-LIF	10~100	30% less than	SFOB	Sadanaga et al., 2004; Yoshino et al., 2006
	Tokyo, Japan	summer, 2006	LP-LIF	10~55	30% less than	SFOB	Chatani et al., 2009
	Tokyo, Japan	spring, 2009	LP-LIF	10~35	22% less than	SFOB	Kato et al., 2011
	Tokyo, Japan	winter, 2007, autumn, 2009	LP-LIF	10~80	10~15 less than	SFOB	Yoshino et al., 2012

Table 1 Total OH reactivity measurements in urban areas (continued)

	Mainz, German	summer, 2005	CRM	10.4		-	Sinha et al.,2008
MEGAPOLI	Paris, France	winter, 2010	CRM	10~130	10~54% less than	SO	Dolgorouky et al., 2012
ClearfLo	London, England	summer, 2012	LP-LIF	10-116	20~40%	SFOB	Whalley et al., 2016
	Lille, France	autumn , 2012	CRM, LP-LIF	~70	Reasonable agreement	SFO	Hansen et al., 2015
	Dunkirk, France	summer, 2014	CRM	10-130		-	Michoud et al., 2015

a. For sources from different studies, the measured reactivity was presented as the averaged results, or ranges of diurnal variations, or the ranges of the whole campaign.

b. For sources of different studies, the calculated reactivity was presented within an uncertainty range, as a percentage reduction or s^{-1} reduction.

c. Measured species that have been used for the calculated reactivity (following Lou et al., 2010): S = inorganic compounds (CO, NO_x, SO_2 etc) plus hydrocarbons (including isoprene); F = formaldehyde; O = OVOCs other than formaldehyde; B = BVOCs other than isoprene;

d. "-" means a lack of information regarding what has been measured or how long it has been measured.

842

843 Table2 Total OH reactivity measurements in suburban and surrounding areas

Campaign	Site	Year	method	$k_{OH(measured)}$ (s^{-1})	$k_{OH\ (calculated)}$ (s^{-1} if it is a value)	Measured Species	Reference
	Central Pennsylvania, US	spring, 2002	LIF-flow tube	6.1		-	Ren et al., 2005
PMTACS-NY2002	Whiteface Mountain, US	summer, 2002	LIF-flow tube	5.6	within 10%	-	Ren et al., 2006b
TORCH-2	Weybourne, England	spring, 2004	LIF-flow tube	4.85	2.95	SFO	Ingham et al., 2009 Lee et al., 2010
CareBeijing-2006	Yufa, China	summer, 2006	LP-LIF	10-30	agree well	S	Lu et al., 2010; 2013
PRIDE-PRD	Backgarden, China	summer, 2006	LP-LIF	10~120	50% less than	S	Lou et al., 2010
DOMINO	El Arenosillo, Spain	winter, 2008	CRM	6.3~85		SF	Sinha et al., 2012
		spring, 2013	CRM	53	23	SFOB	Kumar & Sinha., 2014

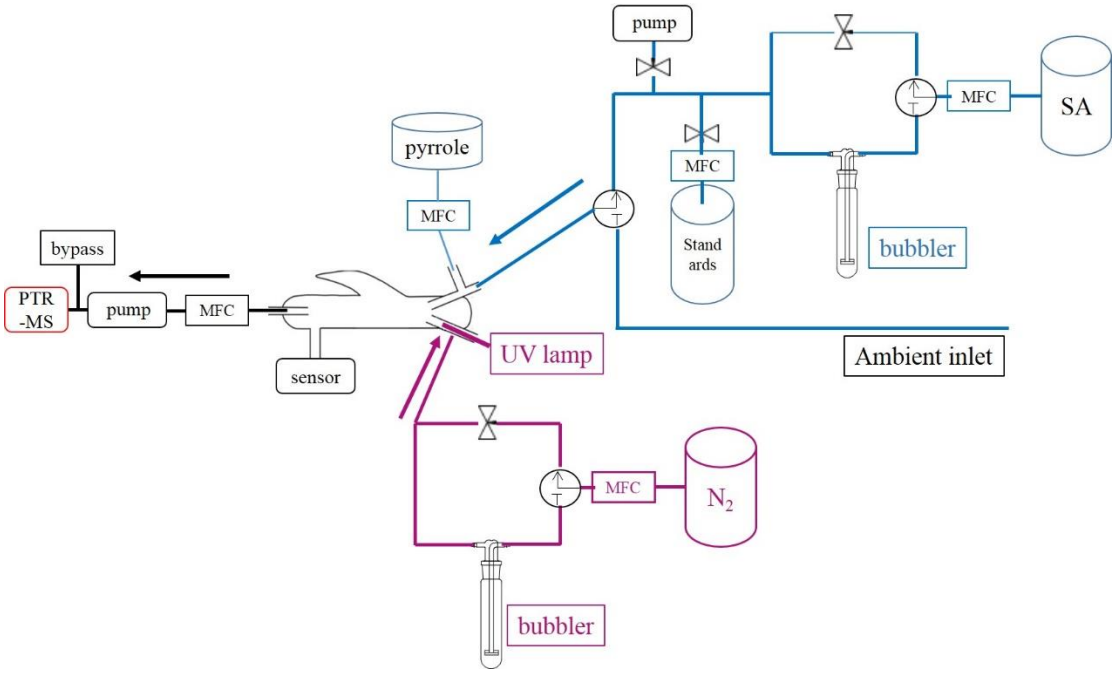

844

845 Fig 1 Schematic figures of CRM system in Beijing and Heshan observations.

846 Blue color represents ambient air or synthetic air injection system, purple color

847 represents OH generating system, black color represents the detection system.

848 Pressure is measured by the sensor connected to the glass reaction.

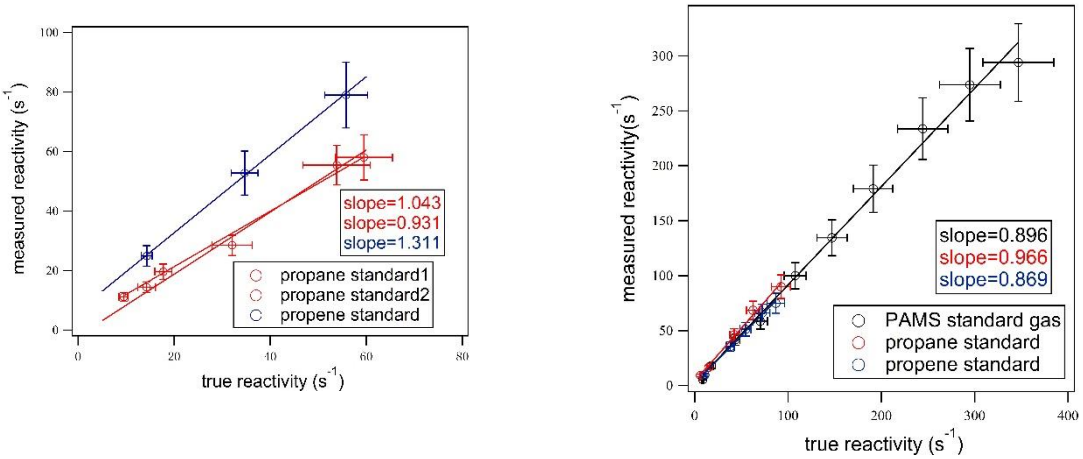

849 Fig 2 OH reactivity calibration in Beijing (left) and Heshan (right).

850 Left: Calibration in Beijing used two single standards: propane, propene;

851 Right: Calibration in Heshan used three standards: propane, propene, mixed PAMS 56

852 NMHCs.

853 Error bars stand for estimated uncertainty on the measured and true reactivity.

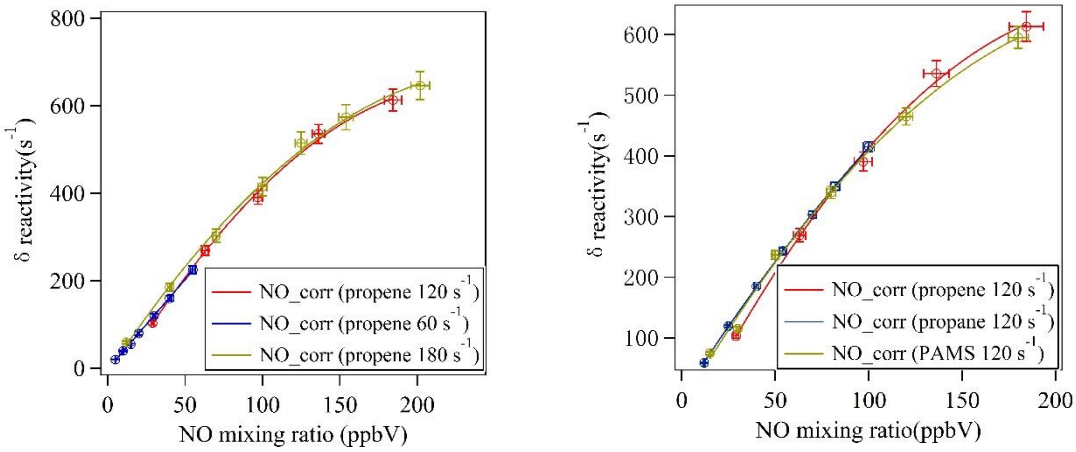

854

855 Fig 3 NO-correction experiments and fitting curves in Heshan 2014.

856 Left: NO-correction experiments with different mixing ratios of propene standard gas;

857 Right: NO-correction experiments with different standard gases at the same reactivity

858 level: 120 s^{-1}.

859 Error bars stand for estimated uncertainty on the NO mixing ratios and difference in

860 reactivity.

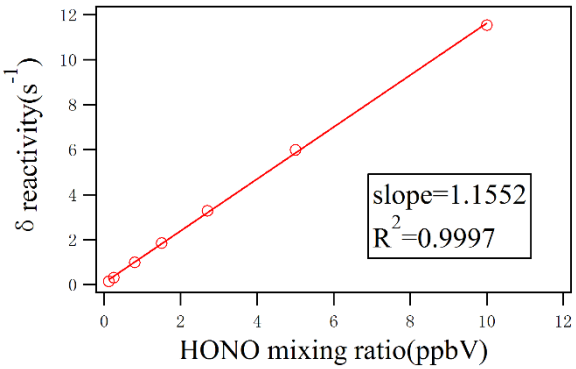

861

862 Fig 4 HONO-correction experiments and the fitting curve in Heshan 2014.

863

864

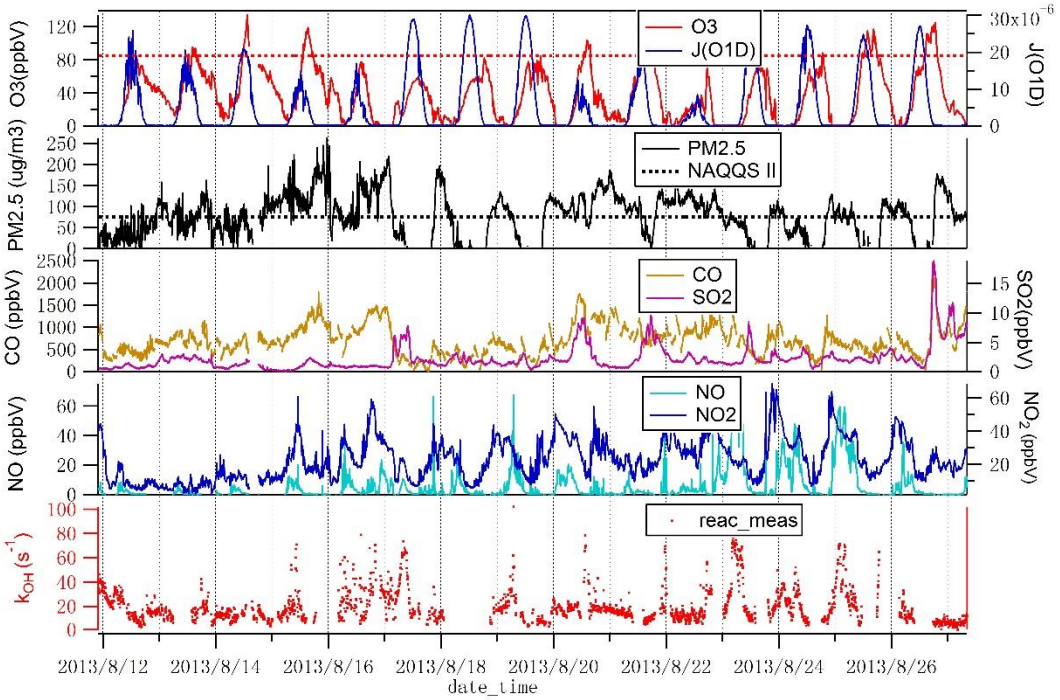

Fig 5-a Time series of meteorological parameters and inorganic trace gases during August 2013 in Beijing.

Red and black dashed lines are Grade II of National Ambient Air Quality Standard.

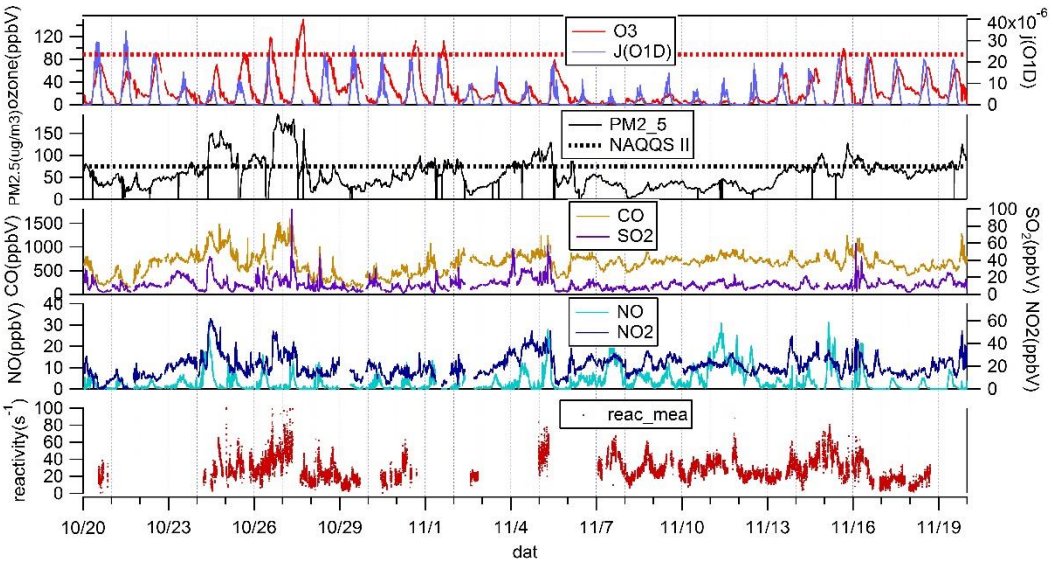

Fig 5-b Time series of meteorological parameters and inorganic trace gases during October-November, 2014 in Heshan.

Red and black dashed lines are Grade II of National Ambient Air Quality Standard.

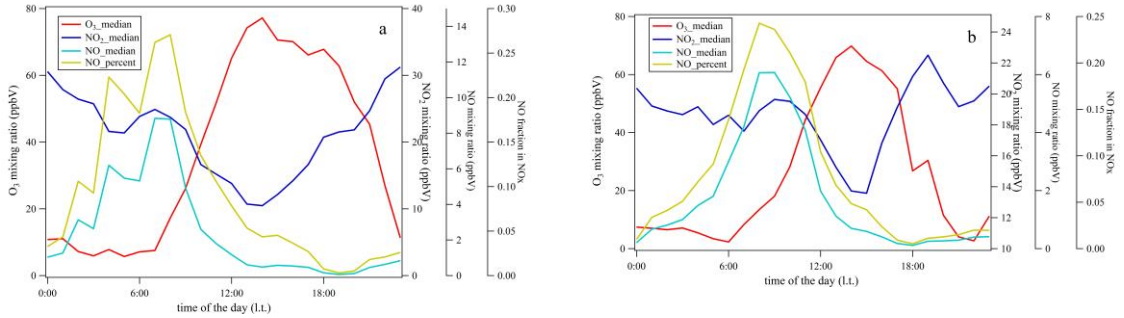

876 Fig 6 Diurnal variations of O_3, NO, NO_2 and relative contribution of NO to NO_x
877 in Beijing 2013 (a) and Heshan 2014 (b)
878

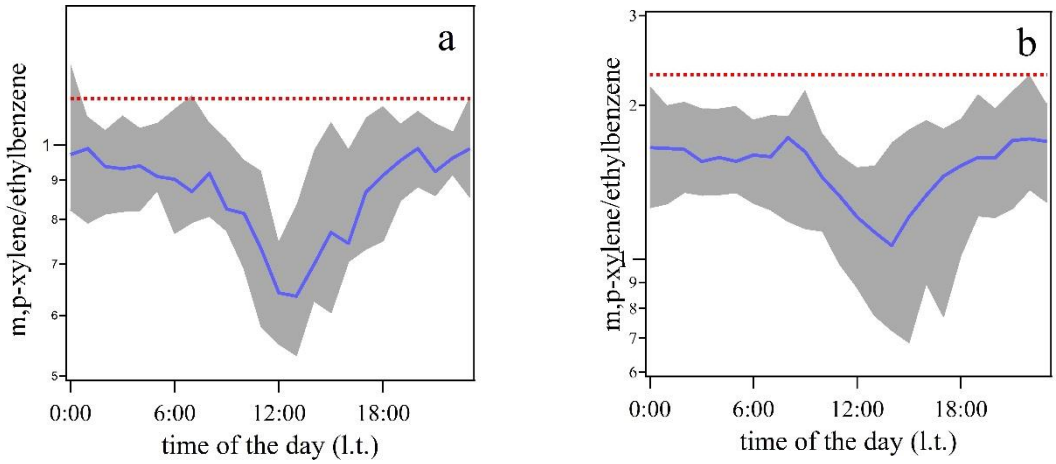

879

880 Fig 7 Ratios of m,p-xylene to ethylbenzene in Beijing 2013 (a) and Heshan 2014 (b)
881 Red dots line: the highest m,p-xylene to ethylbenzene ratio, assumed as emission
882 ratios of m,p-xylene to ethylbenzene, 1.15 ppbV $ppbV^{-1}$ in Beijing 2013 (a) and 2.3
883 ppbV $ppbV^{-1}$ in Heshan 2014 (b).
884 Shaded regions: Standard deviation for the ratios during the campaign average.
885

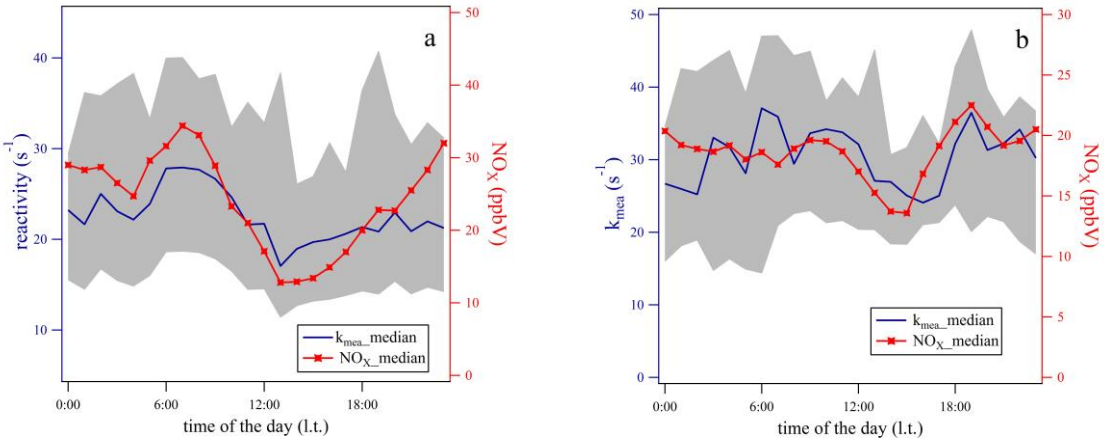

886

887 Fig 8 Diurnal variation of hourly median results of measured OH reactivity and NO_x
888 mixing ratios in Beijing (a) and Heshan (b)

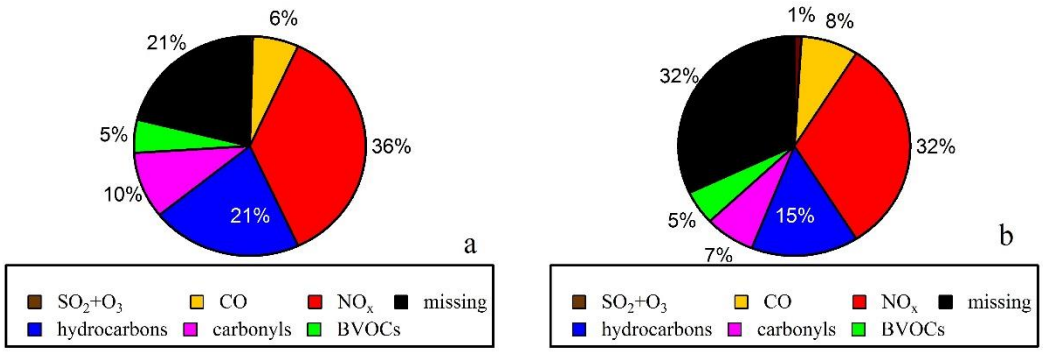

Fig 9 Composition of measured reactivity in Beijing (a) and Heshan (b)

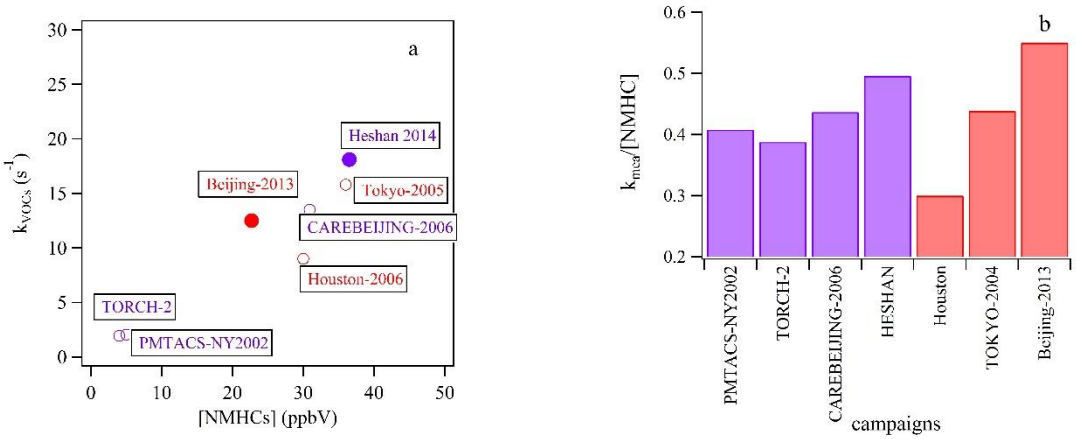

Fig 10 a: Comparison of VOCs reactivity and measured NMHCs in urban and suburban observations.

b: Comparison of the ratio between VOCs reactivity and measured NMHCs in urban and suburban observations

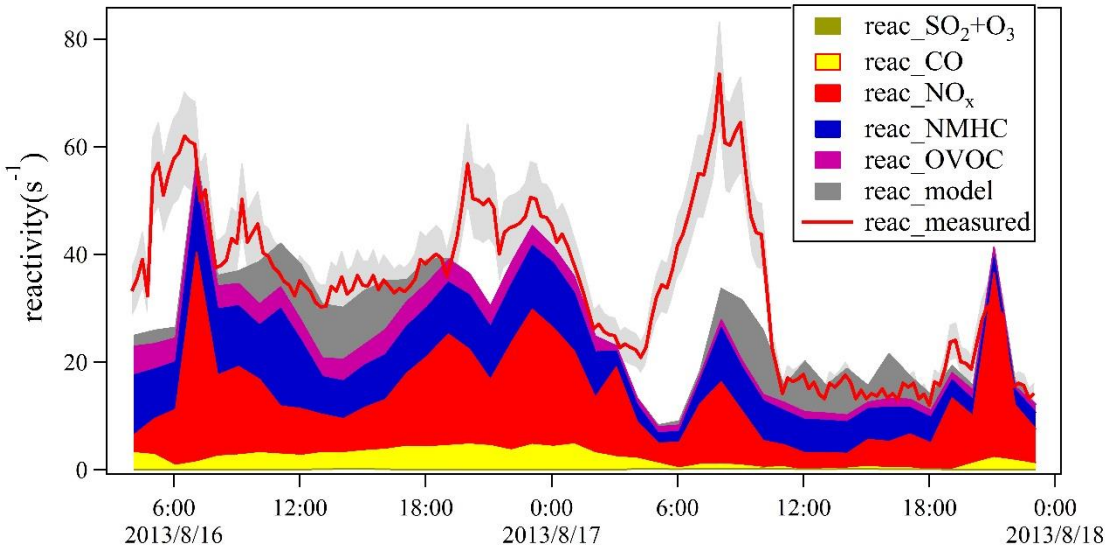

900

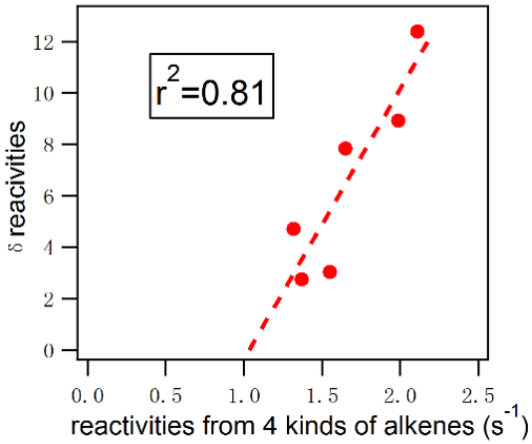

901

902 Fig 11 Upper panel: Comparison between measured and calculated reactivity in
903 Beijing August 16th to 18th 2013.
904 Shallow shaded region: uncertainty of measured reactivity. The same shallow shaded
905 region in Fig 12 represents the same.
906 Lower panel: Correlation between missing reactivity measured in 2013 and reactivity
907 assumed from branched-chain alkenes from 2005 in diurnal patterns. The 4
908 branched-alkenes are iso-butene, 2-methyl-1-butene, 3-methyl-1-butene and
909 2-methyl-2-butene.

910

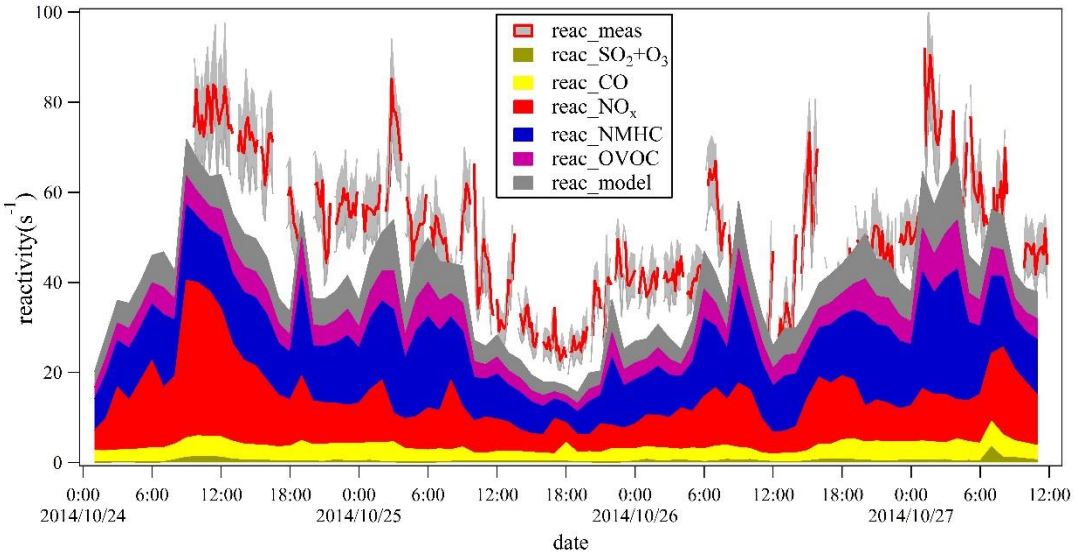

Fig 12 Comparison between measured reactivity and calculated reactivity as well as modelled reactivity in Heshan between October 24th and 27th 2014.

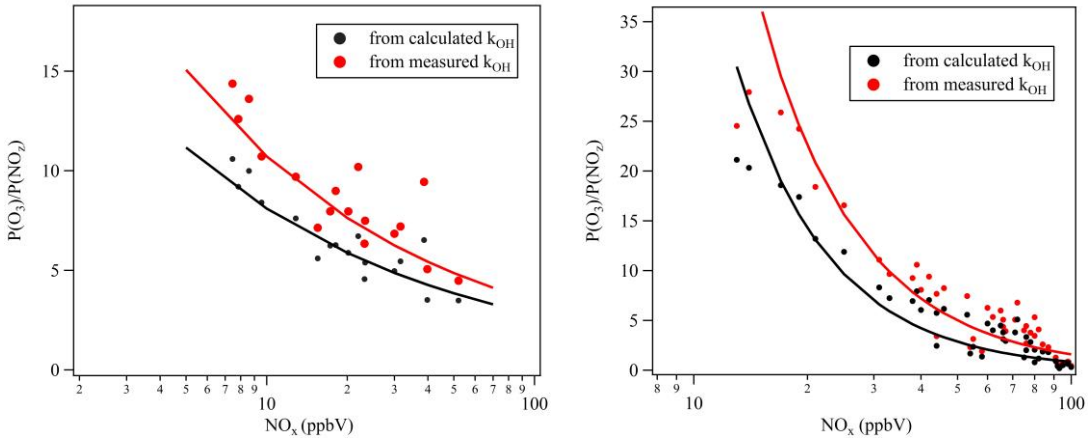

a b

Fig 13 Comparison between OPE calculated from measured reactivity and calculated reactivity in Beijing (a) and Heshan (b).

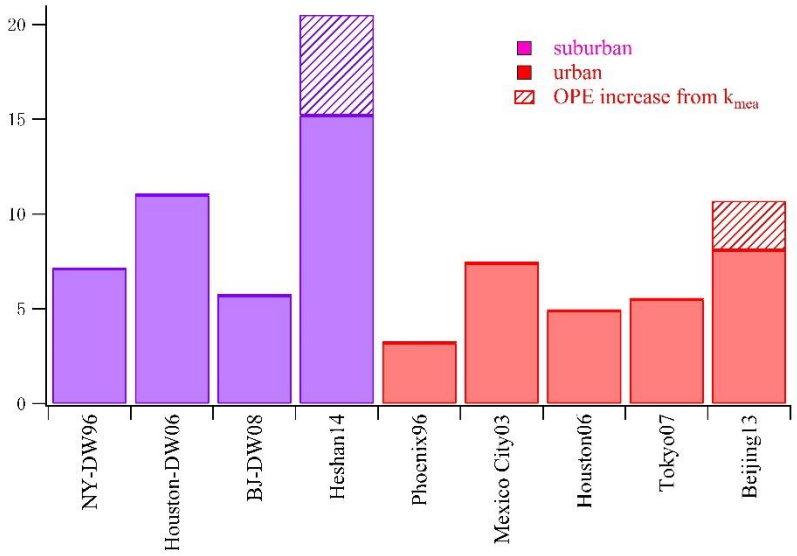

921

922 Fig 14 Comparison between the OPE results in this study and other results from
923 literatures. The comparison is made with the NO_x = 20 ppbV. "DW" is in abbreviation
924 of downwind.

925